

# Development of wet electrostatic precipitator for generation of nanoparticle-protein solution.

Julia Adner 2015

Master Thesis, MAM720

Ergonomics and Aerosol Technology

Faculty of Engineering, LTH

Lund University



Master Thesis

Lunds Tekniska Högskola,  
Ergonomi och Aerosolteknologi, 2015

Author: Julia Adner  
Title: Utveckling av en våt elektrostatisk precipitator för generering av nanopartikel-proteinlösning  
English title: Development of wet electrostatic precipitator for generation of nanoparticle-protein solution.  
Language: English  
Year: 2015  
Keywords: WESP; Nanoparticle; ; biological identity; protein solution  
Citation: Adner, Development of wet electrostatic precipitator for generation of nanoparticle-protein solution. Ergonomics and Aerosol Technology, Faculty of Engineering, LTH Lund University

Ergonomi och Aerosolteknik  
Lunds Tekniska Högskola, LTH  
Lunds Universitet  
Box 118, 221 00 LUND

Ergonomics and Aerosol Technology Faculty  
of Engineering, LTH  
Lund University  
Box 118, SE-221 00 Lund, Sweden

Contents

Acknowledgment	iv
Aeroid – möjlighet till bulkproduktion av guldnanopartiklar i proteinlösning	1
Summary	2
1 Introduction	3
1.1 Background	3
1.2 Aim	5
1.3 Delimitation	5
1.4 Disposition	5
2 Method	6
2.1 Design Approach	6
2.2 Building	10
2.2.1 Material Compatibility Test	10
2.3 Determination of Losses in the System	11
2.3.1 Theory of Diffusion	11
2.3.2 Theory of the Differential Mobility Analyser	12
2.3.3 Method of Loss Measurements	13
2.4 Electrostatic Precipitator Experiments	13
2.4.1 Spectroscopy	14
2.5 Efficiency Experiments	14
3 Results	16
3.1 Determination of Losses Due To diffusion	16
3.2 Electrostatic Precipitator experiment	18
3.3 Deposition Efficiency Experiment	19
3.3.1 Proton Induced X-ray Emission (PIXE)	22
4 Discussion and Conclusions	23
4.1 Discussion	23
4.2 Conclusions	24
4.2.1 Outlook	24
5 References	26

## Abbreviations and Symbols

ESP	electrostatic precipitator
WESP	wet electrostatic precipitator
BSA	bovine serum albumin
Ig G	immunoglobulin G
PBS	phosphate buffered saline
TRIS	tris(hydroxymethyl)aminomethan
Q	flow rate
Z	electrical mobility
Kn	Knudsen number
$x_{rms}$	root mean square distance
N	number of charged particles
$C_c$	Cunningham slip correction factor
E	electrical field
$d_p$	particle diameter
$d_m$	electrical mobility equivalent diameter
$v_e$	migration velocity
$\eta$	viscosity
$\mu$	deposition parameter
$k_B$	Boltzmann constant
D	diffusion constant
e	natural logarithm
SMPS	scanning mobility particle sizer
DMA	differential mobility analyzer
CPC	condensation particle counter
PIXE	proton induced x-ray emission

# Acknowledgment

This project started with discovery and a problem which led to an invention and the invention turned in to the focus of this master thesis.

It has been an interesting, learning and exiting period working with this project. Above all this project has been an experimental and therefore I have learned a lot about practical work in an aerosol lab. But there also have been problems that needed to be solved along the way and these have required precision and a great deal of analysing and planning. I would like to take this opportunity to thank other members that have been a part of this project. First of all I want to thank Christian Svensson that has been my supervisor and the whole project's founder. He has endlessly answered my questions, giving me new ones and supports my decisions along the way.

I would also like to thank the nanometer Consortium at Lunds University, nmC, that has supported this project financially, without them this would not have happened. Other actors involved that I would like to thank is Tommy Cedervall from the Department of Biochemistry and Structural Biology at Lunds University that has provided us with protein solution and Bengt Mueller, Linus Lusvigsson and Maria Messing from Department of Solid State Physics at Lunds University that has provided equipment and knowledge along the way.

Lund, June 2015

# Aeroid – möjlighet till bulkproduktion av guldnanopartiklar i proteinlösning

För att undersöka nanopartiklars toxicitet finns behov av att producera väldefinierade nanopartiklar dispergerade i en kolloid suspension. Men även för andra områden så som nanomedicin finns ett behov av denna typ av lösningar. För att dispergera partiklarna i vätska används ofta ytaktiva ämnen. När dessa ämnen tillsätts adderas de på ytan av partikeln och förändrar partiklarnas yta. Då forskning visar att ytan på en nanopartikel kan spela stor roll för dess effekt i biologiska system har dessa metoders relevans ifrågasatts. Genom deponering av luftburna nanopartiklar direkt på vätska, kan tillsatsen av ytaktiva ämnen undvikas. En ny metod, som innebär deponering på vätska har utvecklats som syftar till att undvika bildandet av en hinna bestående av ansamlade nanopartikel-protein komplex. Partiklar deponeras här på en recirkulerande vätska med hjälp av elektrostatiske krafter och metoden realiserar i en anordning med arbetsnamnet Aeroid. Metodiken tillåter även att större vätskevolymmer med önskvärd koncentration och storlek av nanopartiklar kan produceras vilket ur ett tillämpningsperspektiv är eftersträvänsvärt.

Design av Aeroiden, förlustmätningar av aerosolen och effektivitetsmätningar med avseende på deponering av aerosolen i Aeroiden ingick i metodutvecklingen. Analyser i form av materialval, storlek på vätskevolym samt beräkningar på hur partiklarna förväntas röra sig i det elektriska fältet genomfördes. För att bestämma vilken typ av proteinlösning som skulle användas för att producera en kolloid lösning med 60 nm guldparklar i Aeroiden gjordes referensexperiment, var vid olika proteiner testades vatten och två andra buffertsystem. Den högsta koncentrationen av guldnanopartikel-protein komplex, dvs då vätskehinnan blev som rödast, återfanns då ett blodprotein, albumin, var löst i fosfatbuffert. Denna lösning användes sedan vid de fortsatta testerna av Aeroiden.

Då spänningen var påslagen i Aeroiden deponerades ca 17 % av de luftburna partiklarna. De största förlusterna skedde på grund av partiklarnas diffusion, men vissa förluster kunde även observeras på grund av statisk elektricitet. Som ett komplement till effektivitetsmätningarna bestämdes koncentrationen av guld i vätskan med hjälp av PIXE.

Analys med spektrometri samt visuell inspektion visar att Aeroiden kan framställa 65 ml albuminlösning med dispergerade guldnanopartiklar. Framtida forskning och utveckling borde lägga stor vikt vid analys av hur stor del av partiklarna som är dispergerade för att kunna utvärdera huruvida Aeroiden kan användas för produktion av andra typer av partikel-proteinlösningsskombinationer.

## Snabblexikon:

**PIXE:** står för proton induced x-ray emission. Protoner bombarderas på ett filter med substratet, detta leder till att elektromagnetisk strålning specifik för vart ämne skapas. Denna strålning fångas upp och ger svar på vilka ämnen samt hur mycket av dessa ämnen som finns i substratet.

## Summary

To examine nanoparticle toxicity there is a need to produce defined nanoparticles dispersed in a colloidal suspension. Such a solution could also be interesting for other fields such as nano-medicine. In order to disperse the particles in the liquid there are often surfactant added to the process that alternates the surface of the particles. As the research shows that the surface of a nanoparticle can play a large role of its effects in biological systems, the relevance of these methods have been questioned. By depositing the airborne particles directly in a liquid this mentioned primary treatment can be avoided. A new method for depositing on liquid has been developed that appears to avoid the formation of a film consisting of stagnant nanoparticle-protein complexes. Particles deposited on a recirculating liquid by the means of electrostatic forces, the method is realized in a device named Aeroid. The methodology also allow larger volumes of fluid with relevant concentration. Also the size of nanoparticles can be produced which, from an application perspective, is desirable.

Design, loss measurements and efficiency measurements were included in the method development for the Aeroid. Analyses in the form of materials, volume of the liquid and on how the particles are expected to move in the electric field was performed. For deposition in the Aeroid an aerosol of spherical goldnanoparticles was employed, with size about 60 nm, produced by means of a spark generator in series with a high-temperature-oven. The aerosol is then passed through a bipolar charger to obtain a well known charge distribution. To determine which type of protein solution that could be used to produce a colloid solution with 60 nm gold particles in the Aeroid a control measurements in an ESP where made. There was two types of proteins IgG and BSA added into water, PBS and TRIS. The deposit was made with the same length of time and with the same aerosol concentration for all control measurements. The reddest membrane i. e. the highest concentration of gold nanoparticle-protein complex was found when the BSA was dissolved in PBS. This solution was used for depostion in the Aeroid.

When the voltage with a field strength of 1.2 kV/cm, was applied in the Aeroid 17 % of the produced particles where deposited. It resultled in losses between 13 and 37% at 60 nm, most likely due to diffusion. Efficiency measurements were carried out partly in a SMPS by comparing the penetration of particles in the Aeroid when high voltage was on/off. A complement to the deposition measurement PIXE analysis to determine the concentration of gold in the liquid.

Analysis by spectrophotometry and visual inspection shows that generation of a 65 ml solution of dispersed gold nanoparticles was successfull. Future research and development should put emphasis on the analysis of the proportion of the particles which are dispersed in order to evaluate whether the Aeroid may be used for the production of other types of particle-protein solution combinations.

# 1 Introduction

Nanoscience is believed to be the next thing to revolutionize our lives. Due to their small size and unique properties nanoparticles are attractive to use in a variety of industries from clothes to medicine [1][2]. However, questions regarding how these particles interact with biologic systems still remain largely unanswered. Not only is the field unexplored but the size of the particles makes them hard to control and measure without disturbing the systems or manipulation leading to questionable data. Since more nanoparticles are produced every year [3] there is a need for new methods to better study the interaction between nanoparticles and human, in particular to mimic the reality of the biological interactions.

One specific interaction between nanoparticles and living appears in the alveolar region of the lungs. Because of the small size of the nanoparticles there is a probability that the particles through breathing will end up in the deepest parts of the lungs [4]. The nanoparticles will here through diffusion be deposited on the surface of the alveolar epithelial cells. When reaching this biological setting proteins and other biomolecules immediately adhere to the particles creating a biological identity of the particle [5].

Conventional experiments both *in vivo* and *in vitro* are often performed using a colloidal suspension [6][7]. The suspension is either forced into the respiratory tract of the living animals or the solutions is deposited on to cells. Both these methods deliver the “aerosol” of nanoparticles in a non-biological fluid and the relevance of these experiments have been questioned [8]. In many cases coatings of the particles are necessary to prevent agglomeration in the suspension. This coating changes the surface chemistry and structure of the particle and might also change how a biological environment reacts to it. By deposition of nanoparticles directly onto a biological fluid, letting proteins adhere as they would in nature, a colloidal suspension of nanoparticle-protein complexes can be manufactured [8].

In this thesis a device that seek to manufacture this kind of colloid suspension are presented. In the device with the working name Aeroid particles are deposited through electrostatic forces onto a biological fluid. The biological fluid, in this case a protein solution, recycles to prevent a film formation that occur on top of a biological fluid when exposed to deposition of nanoparticles. This makes the concentration of particle-protein complexes accumulate with time in the whole solution rather than just the air-liquid interface. The process enables the production of customized concentration of nanoparticles, generated in the aerosol form, in a colloidal suspension of a biological fluid.

## 1.1 Background

An aerosol is particles or liquids that are suspended in a gas. These particles can be derived from many different sources such as biological activity, welding and ocean waves. The lifetime in air for the particles depends on its size, shape and ability to interact with other particles or gases [9]. There are approximately about  $10^4$  particles per cubic centimeter at any given moment in a small city (like Lund) [10]. Since the lung is the largest area to the outer world that we have it is no coincidence that there are many diseases related to aerosols, some examples of these are lung cancer and cronic obstructive pulmonary disease [11][12].



## Development of wet electrostatic precipitator for generation of nanoparticle-protein solution

The movements of particles in air are generally controlled by turbulence, gravity (sedimentation) and diffusion (drag force). Particles that are smaller and less dense are less likely to be affected by sedimentation and are therefore more likely to be affected by turbulence and the drag force. Particles less than 100 nm have a longer lifetime in the air and also a greater possibility to follow the air stream into the deeper parts of the lungs although most of the small particles deposit in the head airways. In Figure 1 the diagram shows the size dependent deposition for the different parts of the lungs.

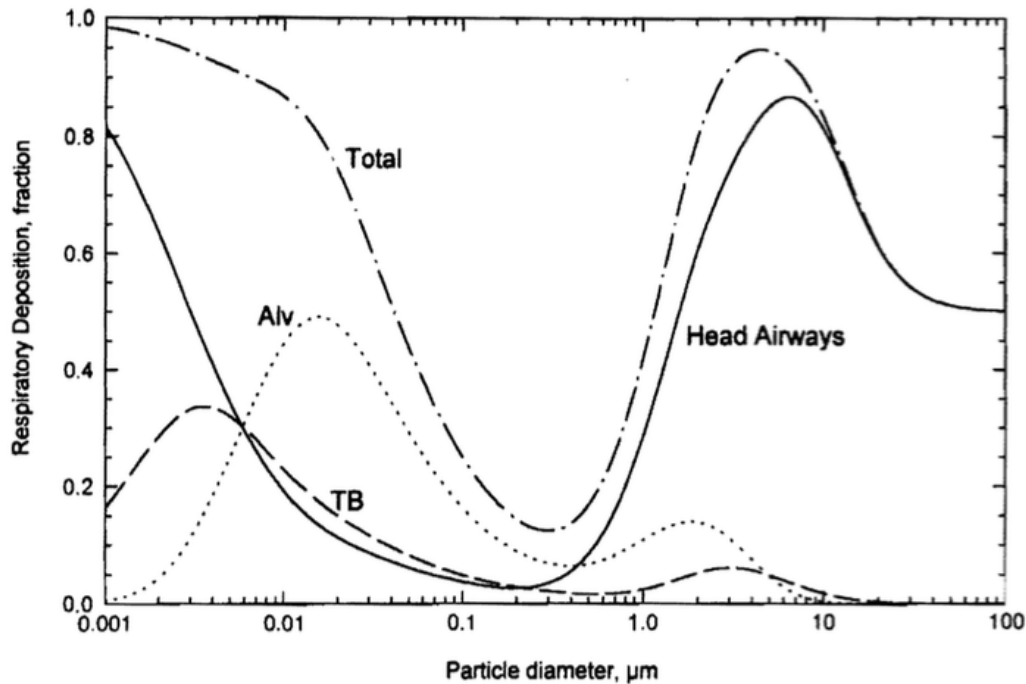


Figure 1 The deposition for particles with diameters ranging from 1 nm to 100  $\mu\text{m}$  for total, head airways, alveolar (Alv) and tracheal bronchial (TB) parts of the respiratory system. [4]

Studies to investigate the toxicity of nanoparticles have been performed [13][14]. In a previous study of this topic Svensson and colleagues have shown that the protein corona of a particle deposited in a solution vary from the particles deposited in an air liquid interface [8]. It has also been shown that the protein corona is important to how the interaction between the cell and the nanoparticles will proceed [15].

Using an electrostatic precipitator (ESP) Svensson with colleagues [8] also discovered that spherical gold nanoparticles formed a film of nanoparticle-protein complexes when deposited in a bovine serum albumin (BSA) solution. This led to the idea of using the ESP technique to produce a solution with desired concentration of gold-protein by constantly breaking the film and permitting the solution to recycle. This idea emerged to the formation of the first version of the Aeroid.

The concept of an ESP, where charged particles are collected/removed from a gaseous environment by electrostatic forces, are not new. Many industries like the coal- and oil-industry use this highly effective system to control emissions. The wet ESP or the WESP is a development where water is used for removal of particles from the electrodes there are also small scale projects that are testing the idea of having a recycling flow to reduce the water consumption [16]. It was argued by Dey and Venkataraman with colleagues [17] that the

possibility of creating a nanoparticle suspension by deposition of particles in a medium would have the advantage of reducing the number of steps and reduce the risk for particle aggregation compared to the conventional way of first collecting nanoparticles in filter and then mixing with a fluid. Another advantage is the fact that a liquid surface are far more elastic so that liquid particles that otherwise might break can be collected. Liu with colleagues [18] showed this when dealing with oils and steric acid particles. The novelty of the Aeroid lies in the fact that the goal is to use the recycling fluid to break the filmformation and by recycling it get the concentration of the particles up to a desired level.

### 1.2 Aim

The focus of this master thesis was in designing, building and evaluating a small scale wet electrostatic precipitator (WESP). The project meant to answer the question: Can a WESP with recycling biological fluid create a colloid suspension >50 ml of protein solution with dispersed nanoparticles with in a time frame of 4 hours? More specific aims were:

- Characterizations of the instruments losses.
- Evaluation of the possibility to use a bipolar charger.
- Evaluation of the deposition efficiency of the Aeroid.

### 1.3 Delimitation

The major demarcation for this project has been the time limit which has led the decision to only study two kinds of particles-fluids combinations: Potassium sulfate particles in water and goldnanoparticles particles in BSA fluid. The project was not intended to produce a commercial product and was always meant to be a small pilot project. It was decided that only one WESP where to be produced and that all changes that required a new WESP is in the outlook of this thesis. The actual use of the fluid has not been considered.

### 1.4 Disposition

This reports is divided into four major parts: introduction, method, results and discussion. In the next chapter, method, a short theory will present the essential concepts that are needed to know to understand this thesis. The technical equipment used and a description of how the experiments were done will also be presented.

The results will be described during part three and finally there will be a discussion together with a conclusion in chapter four.

## 2 Method

The creation and testing of the Aeroid was done in a series of steps from designing and constructing to experiments to evaluate the technique and efficiency. In the chapters below, the steps will be presented and the theory around each subject will be explained.

### 2.1 Design Approach

An ESP (TSI, model 3089) consists of an aerosol inlet, a deposition area and a gas outlet. The particles need to be charged when entering the ESP and therefore a charger is placed before the aerosol inlet. It is important that the devices are designed to charge as many particles as possible with a deposition area that is long enough in relation to the voltage between electrodes. For this both the distance from the inlet hole to the electrode surface, as well as the length of the electrode are crucial.

The aerosol inlet is placed 13 mm from the collecting electrode and approximately 3 mm from the surface of the fluid. Figure 2 shows a schematic view of how particles travel from the inlet into the Aeroid when affected by the electric field. Here the particles are portrayed as positively charged but the electrostatic properties can be varied, as can the direction of the electric field.

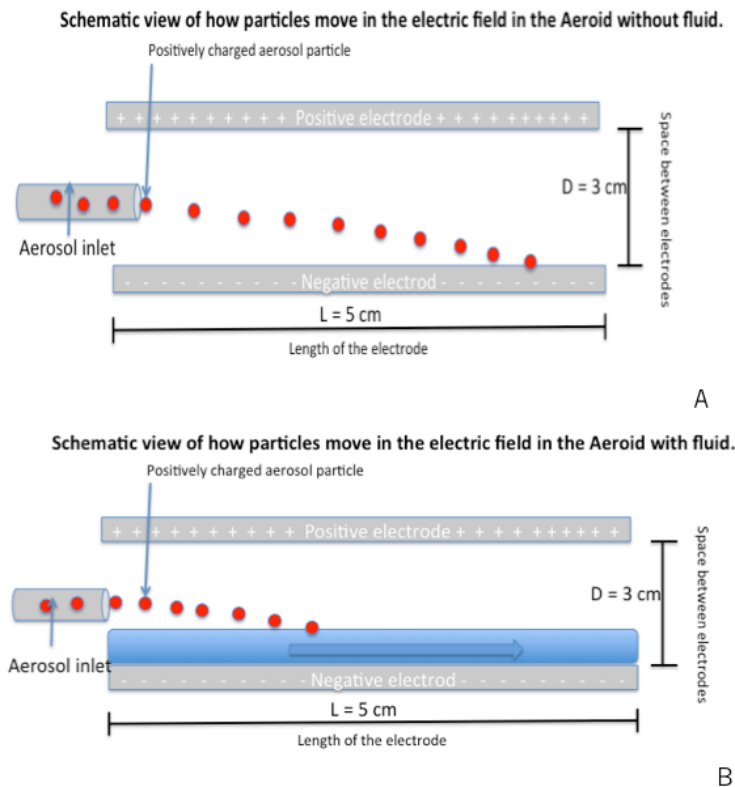


Figure 2 In the top figure (A) a schematic view of how positive particles travel in an ESP when voltage is applied. In the lower drawing (B) the same positively charged particles travels between the electrodes in the Aeroid and deposit in the surface of the fluid instead of the negatively charged electrode

Charged particles move different from uncharged particles in an electric field. The electrical mobility is described by Equation 1.

## Development of wet electrostatic precipitator for generation of nanoparticle-protein solution

---

$$Z = \frac{ieC_c(Kn)}{3\pi\eta d_p} \quad (1)$$

$Z$  is the electrical mobility,  $i$  is the number of charges that a particle carries,  $e$  is defined as the elemental charge ( $e = 1.609 \cdot 10^{-19}$  C),  $C_c$  is the Cunningham slip correction factor,  $Kn$  is the Knudsen number,  $\eta$  is the gas viscosity and  $d_p$  the diameter of the particle.

The Cunningham slip correction  $C_c$  factor is introduced because of the wide span of particle sizes in an aerosol which will influence the interaction of the particles with the gaseous medium. The Cunningham slip direction factor depends on the pressure and temperature of the gas[19].

$$C_c = 1 + Kn \left( \alpha + \beta \exp\left(-\frac{\gamma}{Kn}\right) \right) \quad (2)$$

It has been empirically determined that  $\alpha = 1.142$ ,  $\beta = 0.558$  and  $\gamma = 0.999$  at 1 atm and at 25° C [20]. The Knudsen number is defined as

$$Kn = 2 \frac{\lambda}{d_p} \quad (3)$$

Where  $\lambda$  is the mean free path at 66.4 nm and  $d_p$  the diameter of the particle [21].

When the electrical mobility is disclosed it is possible to calculate the drift velocity  $v_e$ . This can be described as the velocity in which a particle moves towards the electrode of opposite charge, which in the case of the Aeroid, towards the bottom electrode. The migration velocity depends on both the electrical mobility  $Z$  and the strength of the field  $E$  like

$$v_e = ZE \quad (4)$$

Table 1 Calculations of the electric mobility for a 15 nm particle.

$Kn$	8,853
$\alpha$	1,142
$\beta$	0,558
$\gamma$	0,999
$C_c$	15,523
$Z$	9,70E-07 m <sup>2</sup> /Vs
$V_e$	0,113 m/s
$E=V/d$	117000 V/m

At a flow rate  $Q$  of 1.5 l/min which give the residence time for each particle between the plates of 56.5 ms and a total migration distance of 6.38 mm for a particle of 15 nm assuming that it carries only one charge. Particles below 15 nm will not be measured. In the case of the Aeroid the deposition surface is not located on the electrode, but about 10 mm above on the liquid surface. This means that the particles do not need to travel more than a few mm to hit the surface. Eventual voltage losses due to the water resistance were neglected since the particles are not meant to travel further down than to the water's surface. If necessary, the

## Development of wet electrostatic precipitator for generation of nanoparticle-protein solution

equipment allows adjustments for different levels of voltages. The dimensions of the pieces in the Aeroid can be seen in Figure 3.

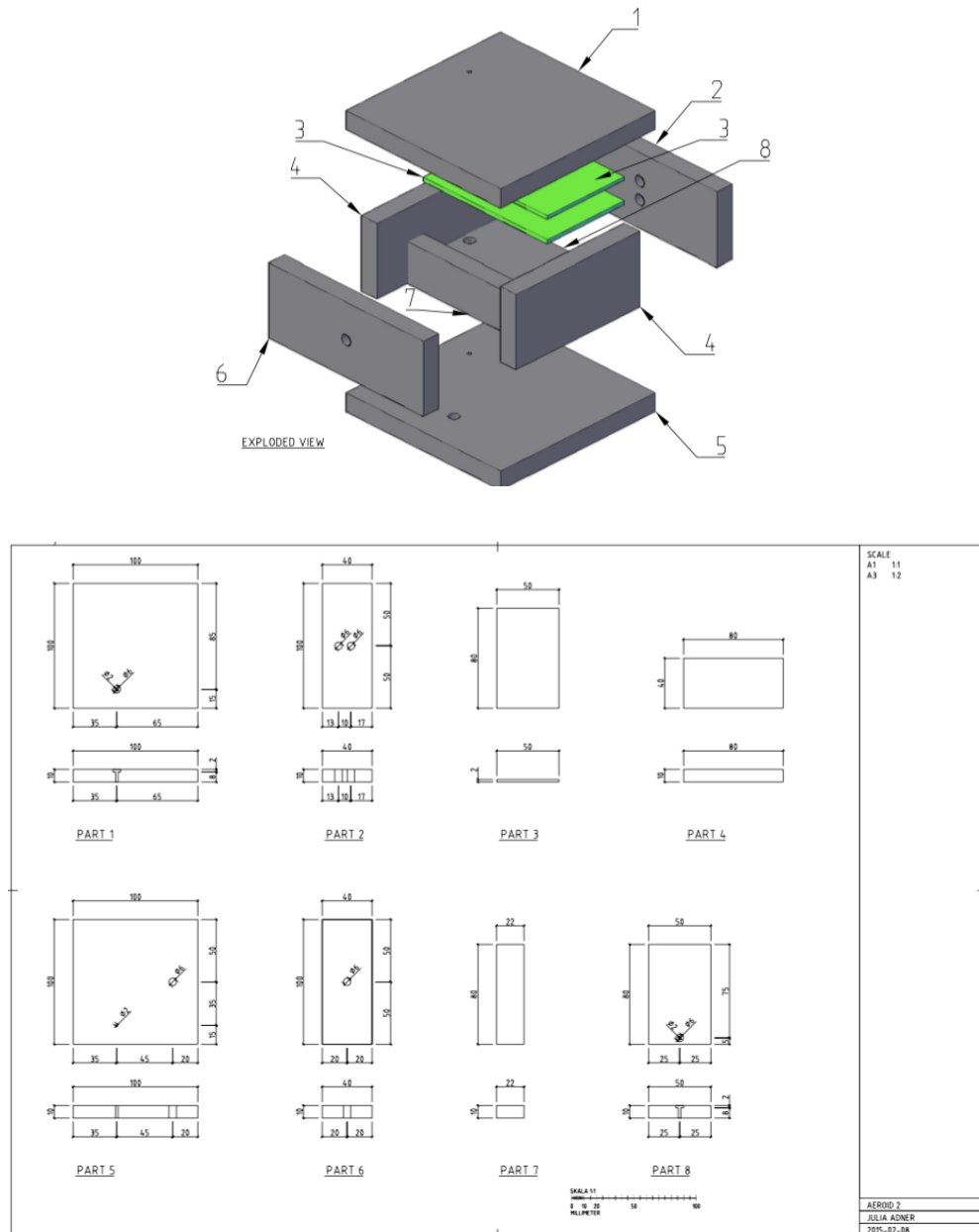


Figure 3. The top figure presents a 3D image of how the individual pieces fit together. On the bottom figure exact measurements of the individual plates are presented. The Aeroid was designed to be cut out of a 1 cm thick poly vinyl chloride board.

One further aspect of designing the Aeroid were the amount of circulating fluid. The aim was to have 65 ml of recycling fluid which the voids were designed to fill. The large basin contains 40 ml while the small basin have a bottom of 16 cm<sup>2</sup>. Thus when filled with up to 0.5 cm contains 8 ml. The tubes have the length of 40 cm this includes the volume that goes in to the pump, and hold about 8 ml. The pump (Autolude, model EV 500) used for moving the liquid around has maximum capacity of pumping 83 ml/min. In Figure 4 a schematic view of how the liquid circulates in the Aeroid is presented.

## Development of wet electrostatic precipitator for generation of nanoparticle-protein solution

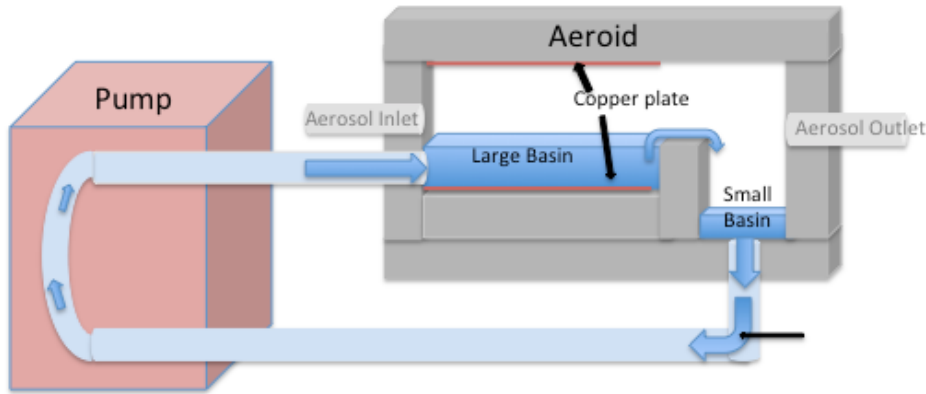


Figure 4 Schematic view of how the pump moves the fluid in the Aeroid to create a constant overflow between the large basin and the smaller basin.

One of the most important features regarding deposition efficiency is the possibility to charge the particles. In this case it is important to deposit the particles on to the surface of the liquid ergo, with the same charge to the greatest extent as possible.

The bipolar charger ionizes the gas phase in the aerosol by  $\beta$ -radiation from a radioactive force, in this case Kr85. The number of charges per particle is dependent on the particle diameter. Equation 5 describes the relationship:

$$f(N) = 10^{(\sum^5 a_i(N) \cdot (\log(\frac{D_p}{nm})^i))} \quad (5)$$

$N$  is the number of charges at a particle,  $D_p$  the diameter in nm and  $a_i$  is the Wiedensohler coefficient. This equation originates from the Gunn [22] and Fuchs theory [23] and is a development of Wiedensohler's earlier work (1988) [24]. The expected charge distribution is presented in Figure 5, it shows that about 26 % will have a negative charge at 60 nm and about 16 % at 30 nm. The fraction that will have a positive charge at 60 nm will be around 20 % and about 13 % will have a positive charge at 30 nm. The rest of the particles will have zero charge and will not be deposited through electrostatic forces.

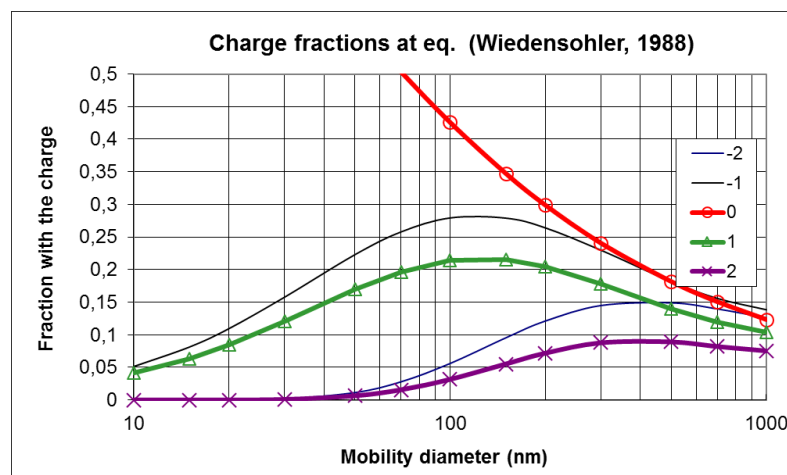
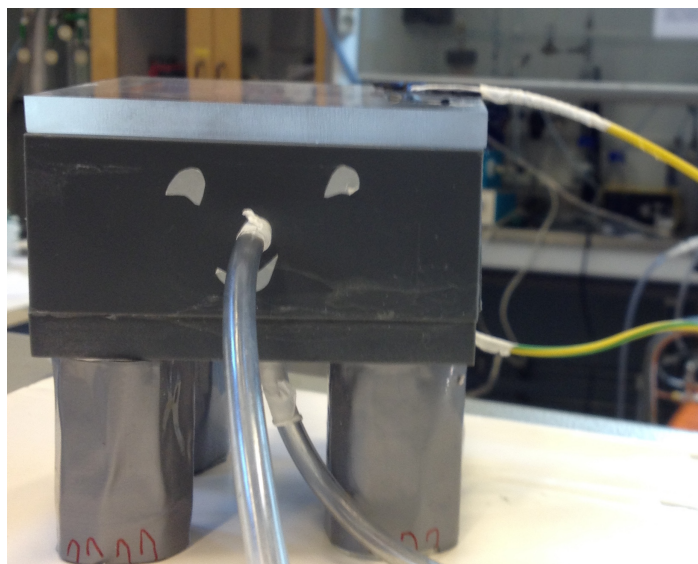


Figure 5 Boltzmann-Fuchs charge distribution for particles with mobility diameter ranging from 10 nm to 1  $\mu$ m [4]

## 2.2 Building

The Aeroid was built in polyvinyl chlorid (PVC) with a lid of plexiglas. The pieces was cut out of a 10 mm thick PVC sheet. The end result is presented in Figure 6.



*Figure 6 The Aeroid, here with legs of duct taped plastic foam and a PVC body and the Plexiglas lid. The tubes visible are the aerosol outlet at the front and the liquid outlet at the bottom. The wires connected to a high-voltage unit protrude from the lid and the bottom.*

The pieces were glued together as shown in Figure 3. Because of the purpose for the Aeroid it is important that it is water and air tight. The joints were sealed with silicone on the inside and the tubes made of tygon plastic were sealed with teflon tape. To be able to stay totally air tight vacuum grease were applied on the edges of the lid before each experiment. It was also washed with acetone, ethanol and distilled water in that order afterwards. By connecting a filter to the aerosol inlet and the outlet to the particle counter, measurements were done before each experiment to make sure that there was no leakage.

### 2.2.1 Material Compatibility Test

Experiments to test the protein reaction to the materials used in the Aeroid was investigated. The proteins tested were bovine serum albumin (BSA) and Immunioglobulin G (IgG) mixed separately in water, phosphate buffered saline (PBS) with 7.5 pH and tris(hydroxymethyl)aminomethane (TRIS) with 7.5 pH. Each protein solution were tested with copper, PVC and silicone. The test subject was placed in a vial and a small amount of the protein solution was poured in. The vials were initially shaken and left over night. The following day, the vials were tested for precipitation by checking the clarity of the solution by use of microscope. Since none of the vials showed signs of protein precipitation or other disturbance one could conclude that the material chosen would not affect the samples.

## 2.3 Determination of Losses in the System

When dealing with an aerosol losses will occur due to different mechanisms like diffusion, sedimentation and impaction. In these experiments the produced particles will have a measured diameter with a normal distribution around 30 or 60 nm and a range from 15 nm to 300 nm.

### 2.3.1 Theory of Diffusion

The motion and loss of particles in the size range is primarily described by diffusion and brownian motion. Brownian motion is the net result of the random movement of particles due to collision with the surrounding gas molecules. This is because larger particles will interact with the gas as it were a continuum media while particles under 0.1  $\mu$ meter [4] will recognize each molecule that bounce and therefore be more susceptible to the high velocity of the gas molecule making the particle move in a randomized motion. To be able to calculate how far, in average, that a particle moves due to these collisions a *root mean square distance* ( $x_{rms}$ )

$$x_{rms} = \sqrt{2Dt} \quad (6)$$

can be calculated. Where  $D$  is the diffusion constant and can be described by equation (7):

$$D = \frac{(C_C k_B T)}{3\pi\eta d} \quad (7)$$

$k_B$  is the Boltzmann constant,  $T$  is the temperature in Kelvin,  $\eta$  is the viscosity of the surrounding medium in this case air ( $1.822 \cdot 10^{-5}$  kg/(m·s)) and  $d$  is particle diameter [19]. In order to calculate the losses in tubes equation (8) can be used (Hinds Brownian motion and Diffusion).

$$P = 1 - 5,5 \cdot \mu^{\frac{2}{3}} + 3,77\mu \quad (8)$$

This is a simplified equation that gives a good estimate to losses by diffusion.  $P$  is the penetration function and  $\mu$  the dimensionless deposition parameter given by equation (9) assuming laminar flow.

$$\mu_1 = \frac{DL}{Q_s} \quad (9)$$

Where  $L$  is the length of the tube and  $Q_s$  is the flow rate [4]. Since particles below 0.1  $\mu$ m primarily are subjected to losses due to diffusion, losses connected to sedimentation are neglected for this thesis [19].

Other losses that are harder to theoretical foresee are losses owed to electrostatic forces. Losses due to both diffusion and electrostatic forces are measured in the Aeroid with a scanning mobility particle sizer (SMPS). The SMPS used are an inhouse built system that contains a bipolar charger, a differential mobility analyser (DMA, TSI Inc., model 3071) and a condensation particle counter (CPC, TSI Inc., model 3775).



### 2.3.2 Theory of the Differential Mobility Analyser

The basic principle for a DMA is that a laminar flow of an ionized aerosol is introduced into a gap between two cylinders. The flow of the aerosol is kept along the sides of the outer cylinder. A sheath of clean laminar current of air flows between the aerosol and the inner cylinder. When a voltage is applied on the inner cylinder an electrical field  $E$  is introduced:

$$E = \frac{V}{r \cdot \ln\left(\frac{R_2}{R_1}\right)} \quad (10)$$

$V$  is the potential,  $r$  is the radius of the particle and  $R_1$  and  $R_2$  is the radius of the inner and outer cylinder, here 0.00937 cm and 0.01961 cm respectively (Flagan 2001). The strength of the field controls which particles will pass in to a slit along the inner cylinder that has the characteristic length of 0.4437 cm. These particles will then pass through to a CPC. The aerosol particles that do not pass over the sheath airflow will be lead to a filter. The particles that are within the range and pass over the clean air but not into the slit will deposit on the inner cylinder. As mentioned before the number of charges depends on size of the particle. A large particle will have a probability (equation 4) to accumulate more charges.

The DMA measures particle diameter with respect to the electrical mobility diameter  $d_m$  due to the charge of the particle. In equation 9 the relationship between the electrical mobility and the  $d_m$  can be seen.

$$d_m = \frac{ieC_c}{3\pi\eta Z} \quad (11)$$

The software in the SMPS divides the scan in to intervals and controls the DMA. For each slot that contains a normal distribution of particles a midpoint diameter is calculated. For each diameter interval that goes in to the CPC, the CPC counts the particles in each slot making a sum of all the particles in this interval. The CPC consist of a heated alcohol reservoir that evaporates into the aerosol. The heated aerosol is then cooled in a condenser chamber where the alcohol condenses on the particles. This makes the particles “grow” in diameter and easier to be detected by the laser beam when the particles passes through a small slit on the way to the filter. A photo detector converts the number of disturbed signals into electrical pulses. The CPC have a vacuum pump that draws 1,5 lpm. The set up used for loss measurements is presented in Figure 7.

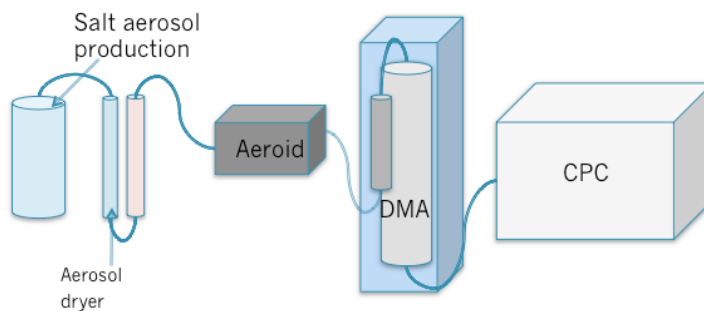


Figure 7 Schematic setup of the units connected in the particle loss measurements. A TSI Nebulizer produced a potassium sulfate aerosol. The aerosol is then sucked by the vacuum pump in the CPC through a bipolar charger, the Aeroid and the SMPS, which consist of a DMA, TSI Inc., model 3071 and a CPC, TSI Inc., model 3775.

# Development of wet electrostatic precipitator for generation of nanoparticle-protein solution

## 2.3.3 Method of Loss Measurements

Loss measurements for diffusion and static electricity were done for the Aeroid, the bipolar charger and the two together were done with potassium sulfate aerosol that had a gaussian looking distribution around 32 nm and a top concentration of  $10^6$  particles/cm<sup>3</sup>. The sulfate aerosol was generated by a TSI Nebulizer in both of the occasion.

Diffusion was measured by first connecting the aerosol flow directly into the SMPS, this was done to get a reference value. Then the Aeroid and/or the bipolar charger were connected. Each measurement where done by a set of 4 scans on the SMPS before changing parameters followed by calculation of the average for each measurement. An estimation of losses based on data from the SMPS system will be calculated trough:

$$\frac{P_{Without\ Aeroid} - P_{With\ Aeroid}}{P_{Without\ Aeroid}} = \text{Fraction particles losses in the Aeroid} \quad (12)$$

$P_{Without\ Aeroid}$  are the number concentration of particles in a diameter interval that prenetarte when the Aeroid not is conncteted to the SMPS system,  $P_{With\ Aeroid}$  are the number concentration of particles in a diameter interval that penetarte the Aeroid.

## 2.4 Electrostatic Precipitator Experiments

Measurements with the ESP (TSI, model 3089) were performed to determine what protein to use in the Aeroid. 100  $\mu$ l were placed in a petri dish with 50 mm in diameter and put in the ESP for one hour.

When nanoparticles deposit on the surface of a biological solution a corona will form when biomolecules and proteins that associates to the surface of the particle. The corona is dynamic and will change, although equilibrium will be reached during time. The biological identity of the particles will depend upon the particle size, surface structure and material [25]. However the formation and behavior of these coronas are not yet fully understood. The idea is to use the corona formation, where each gold particle is separated by the cover of proteins keeping the particles un-agglomerated while simultaneously receiving their biological identities.

BSA is one of the proteins that most easily attaches to the surface of a particle [25] and are the main portein in blood plasma in cows [26]. IgG, produced by B-lymfocyt, is the most common antibody type in our vascular system and is mainly released to control infections [27]. In Table 2 the doses of the proteins in water, PBS and TRIS are presented.

*Table 2 Bovine serum albumin (BSA) and Immuniogloblin G (Ig G) was separatly mixed with water, phosfate bufferd saline (PBS) and tris(hydroxymethyl)aminomethane in the concentartions presented bleow.*

	H <sub>2</sub> O	PBS	TRIS
BSA	3,4 mg/ml	30 mg/ml	30 mg/ml
Ig G	35 mg/ml	34 mg/ml	34 mg/ml

The spark generator used (Palas GmbH, model GFG-1000) two rods of gold are placed in a plastic chamber. When a high voltage is applied sparks arrise between the rods causing the

## Development of wet electrostatic precipitator for generation of nanoparticle-protein solution

vapor that is produced in the spark to condense into particles. By controlling the carrier gas flow (nitrogen in this case) and the voltage applied it is possible to adjust the sizes of the particles generated. If the pressure is high from the carrier gas, the vapor is quickly removed from the chamber and cooled down which makes for smaller particles. If the voltage is high more fume are produced, leading to more particles. The pressure used was 0.3 bar +/- 0.1 bar and the voltage applied was at 0.9 kV to 1 kV.

The spark generator is connected to an oven (Gental Signal Lindberg) that sinters the agglomerated particles that come from the spark generator. The oven is a and were set at 806 °C. The set up can be seen in Figure 8.

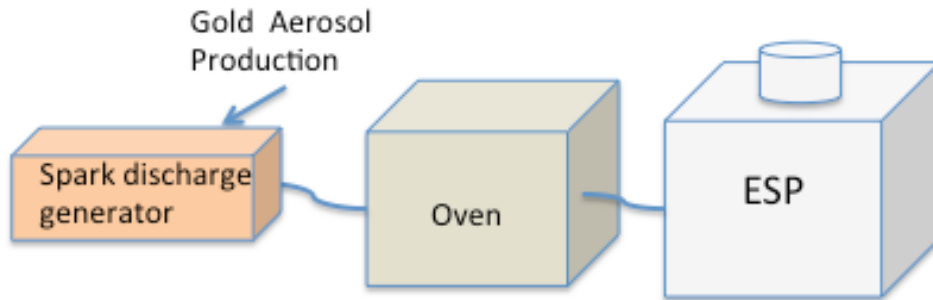


Figure 8 A schematic overview of the set up in the electrostatic precipitator experiments. The Palas GFG-1000 produced a gold aerosol, the particles were then sintered in the Gental Signal Lindberg high-temperature oven to be deposited on the samples in the ... ESP.

To be able to determine what sizes of particles that would go in to the ESP, measurements with the SMPS were done before and after deposition with the ESP.

### 2.4.1 Spectroscopy

A compliment to visual studies of the samples spectroscopy was used to measure the absorbance of light from 200 – 1000 nm with Thermo Scientific model Multoskan Go [28]. A beam of electromagnetic radiation with a certain intensity  $I_{incident}$  are directed at the sample, the intensity of the transmitted radiation  $I_{transmitted}$  is then measured to give the absorbance [29].

$$\frac{I_{incident} - I_{transmitted}}{I_{incident}} = Absorbance \quad (13)$$

Goldnanoparticles in the particle size up to 100 nm absorbs light in the range of 450 nm – 700 nm, depening on size, shape and adsorbants [30]. That means that a peak in this wavelenght range would confirm the presence of dispersed goldnanoparticles.

## 2.5 Efficiency Experiments

Efficiency in an ESP and therefore also in the Aeroid is defined as how large percentage of the particles is collected onto a desired substrate. The Deausch-Anderson Equation [31] gives an estimate that is based on the ideal conditions:

$$\tau = 1 - e^{-v_e \left(\frac{A}{Q}\right)} \quad (14)$$

## Development of wet electrostatic precipitator for generation of nanoparticle-protein solution

---

Where  $\tau$  is the collection efficiency of the precipitator,  $e$  is the base of natural logarithm,  $v_c$  the migration velocity,  $A$  the area of the collecting plates and  $Q$  the gas flow. This assumes equal flow rate over the whole precipitation area and equal migration velocity for all sizes of particles. However, this is not true as Equation (3) and (4) states that the number of charges increases with increasing size. Thus, this increases the mobility  $Z$  and therefore also the migration velocity  $v_c$ . The problem of dust affecting the collection efficiency can here be neglected, as the Aeroid does not collect particles on the electrodes but on the surface of the liquid. The true collection efficiency in the case of Aeroid would instead be to measure the concentration of particles in the liquid. There are a number of ways to measure the concentration of gold in protein solutions but because of lack of time this project has to rely on the capability of the SMPS to measure the differences in size from having the Aeroid deposition on/off. An estimated efficiency based on data from the SMPS system will be calculated through:

$$\frac{P_{0V} - P_{3.5kV}}{P_{0V}} \cdot \frac{1}{2} = \text{Fraction deposited particles in the protein solution} \quad (15)$$

$P_{0V}$  are the number concentration of particles in a diameter interval that penetrate the Aeroid when the high-voltage unit is shut off,  $P_{3.5kV}$  are the number concentration of particles in a diameter interval that penetrate the Aeroid when the high-voltage unit is on at 3.5 kV. The expression is divided with two because only one of the electrode residence below the liquid surface therefore only about half of the charged particles will be deposited in the liquid as seen in Figure 5.

A schematic view is presented over the arrangement in Figure 9. This experiment started and ended with one set of three runs with the SMPS without the high-voltage applied in the Aeroid.

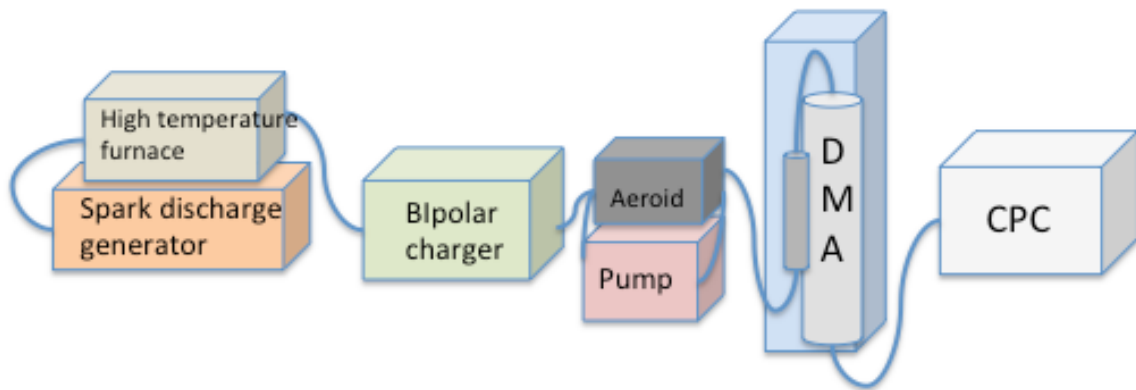


Figure 9 A schematic presentation of the setup of the efficiency experiments. The Palas GFG-1000 produced a gold aerosol; the particles were then sintered in the Gentel Signal Lindberg high-temperature oven. The sintered gold aerosol particles were lead through a bipolar charger to be deposited in the Aeroid. The particles that were not deposited penetrated the Aeroid into the SMPS consisting of a DMA and a CPC. The pump was used to move the protein solution in the Aeroid as shown in Figure 4.

## 3 Results

### 3.1 Determination of Losses Due To diffusion

Since the particles generated, salt- and goldnanoparticles, have a lognormal distribution around 30 nm and 60 nm respectively, losses due to diffusions will occur in the tubes connected from the bipolar charger to the Aeroid and further to the SMPS. To be able to understand what fraction that would penetrate the tube Eq. 6-8 were used to calculate the losses for each particle size between 15 to 600 nm. Figure 10 shows the result from the calculations. It is calculated for a 1 m tube with a flowrate at 1.5 l/min and a tube diameter of 6 mm which corresponds to the settings during experiments. As expected the fraction losses are greater for small particles. At 30 nm the efficiency is at 98% and at 60 nm at 99%. For this experiment the losses in the tubes has little effect on the end result but should be considered in future work, since large aerosol penetration could mean build up in both tubes, oven and in the Aeroid.

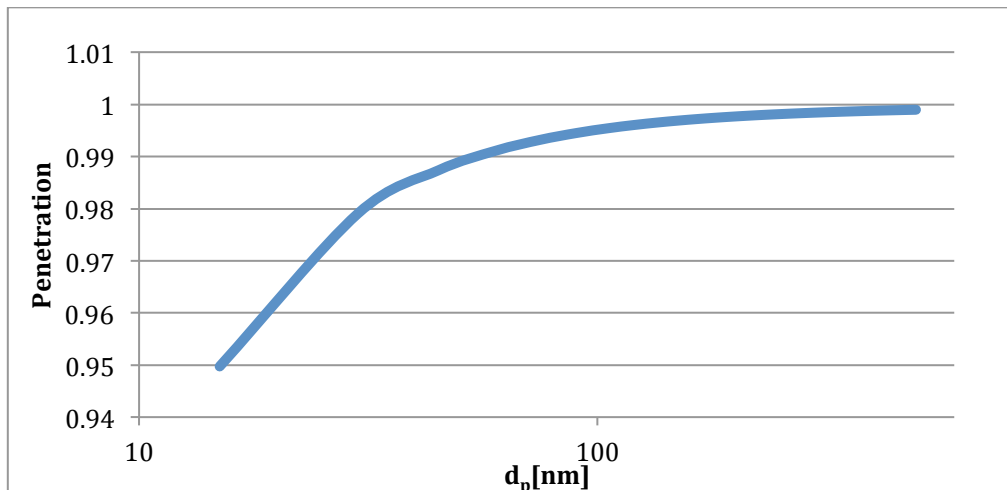


Figure 10 Penetration calculations done using Eq. 6-8 for each particle diameter for a 1 m tube with a diameter of 6 mm.

Losses due to diffusion in the Aeroid was also investigated. This was done at two separate occasions, one with a mode diameter at 30 nm, another with 2.2 times higher particle count than the first and further a mode diameter at 40 nm. The set up can be seen in Figure 6. On both occasions potassium sulfate aerosol was employed. Eq. 12 was used on the the size distributions from both of the occaseion in each paticle diameter interval to give Figure 11. In Figure 11 a large percentage of losses for all particle sizes can be seen. The losses increase by decreasing particle diameter and is caused by diffusion losses. While the data represented by “Mode d. 40 nm” in Figure 11 for most parts corresponds to the expected results that the losses for diffusion are largest at small particle sizes. The data represented by “Mode d. 30 nm” in Figure 11 shows a slight U-formed curve. Since the particle count is rapidly decreasing after 100 nm, the anomaly could be due to sudden disturbance in the system or inconsistency of aerosol production. However it is also possible that greater fraction losses could occur with higher concentration i.e. the losses colud be concentration dependent. In “Mode d. 40 nm” a small dip between 16 and 22 nm is seen, this could be explained by the same mechanisms

## Development of wet electrostatic precipitator for generation of nanoparticle-protein solution

described for “Mode d. 30 nm”, since “Mode d. 40 nm” have a lognormal distribution around 40 nm, few particles are produced below 20 nm.

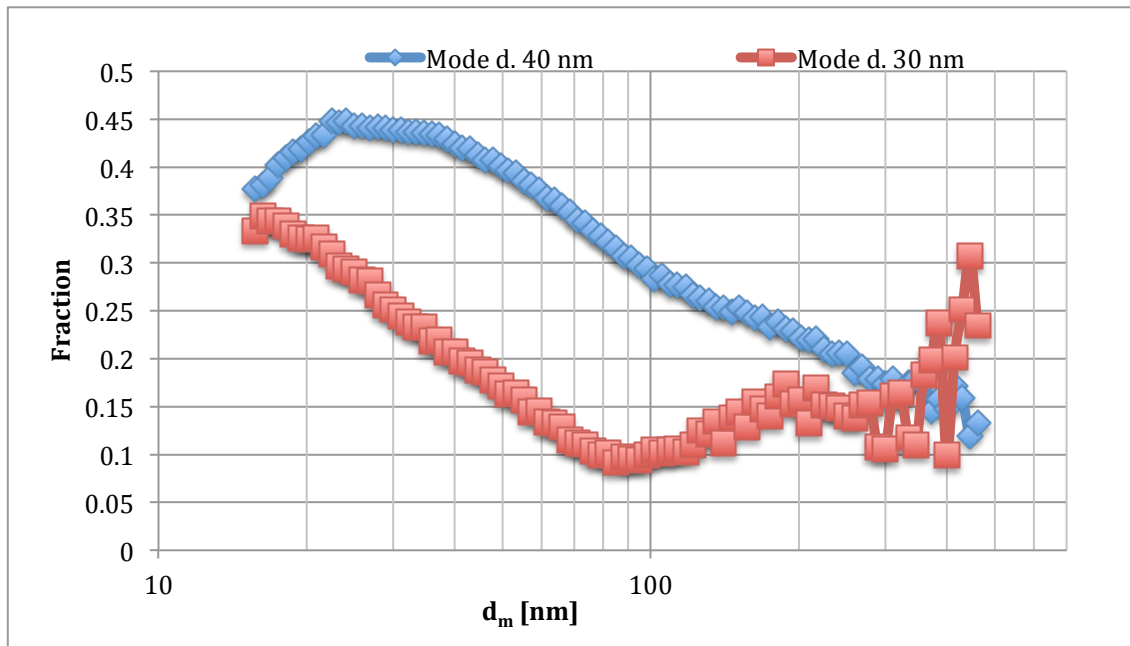


Figure 11 Losses due to diffusion in the Aeroid for two different measurements. “Mode d. 40 nm” has a 2.2 higher particle concentration than “Mode d. 30 nm” and a particle lognormal distribution around 40 nm. “Mode d. 30 nm” has a distribution around 30 nm.

The deposition due to diffusion could be seen as a fine pink layer in tubes and also in the Aeroid upon cleaning. Figure 12 displays the diffusion and static electricity losses occurring when the bipolar charger is connected. Due to inconsistencies in the aerosol production and because of above mentioned causes when there are few particles per size interval, the values are going down below zero at 44 nm. Although not clear this image showed that losses are small in the bipolar charger.

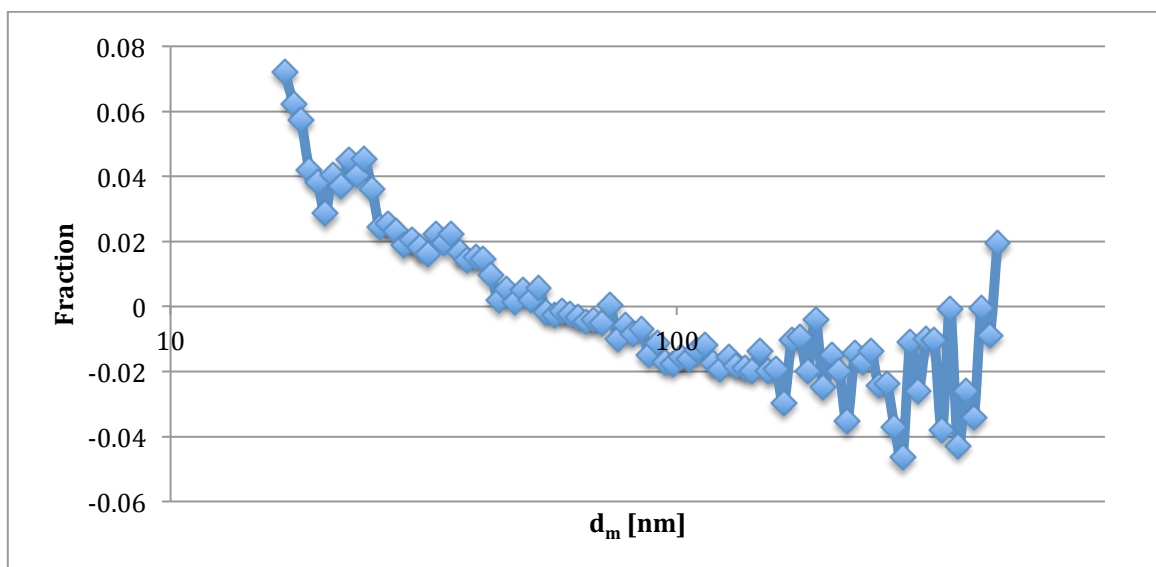


Figure 12 Losses due to diffusion and electrostatic effects in the bipolar charger.

### 3.2 Electrostatic Precipitator experiment

Experiments were done with six samples containing different combinations of buffer and proteins to investigate what solution to use in the Aeriod. It is important to know that a protein corona is formed around a single gold nanoparticle to keep them separated from each other. Because gold nanoparticles emit light in colors from violet to red depending on the size, it is relatively easy to tell if the particles are dispersed in a solution or not.

A gold aerosol produced by a spark generator with a distribution around 60 nm was used. At 10 kV and with a gas flow of 1.5 l/min each sample was deposited upon for one hour. The results are presented in Figure 13.

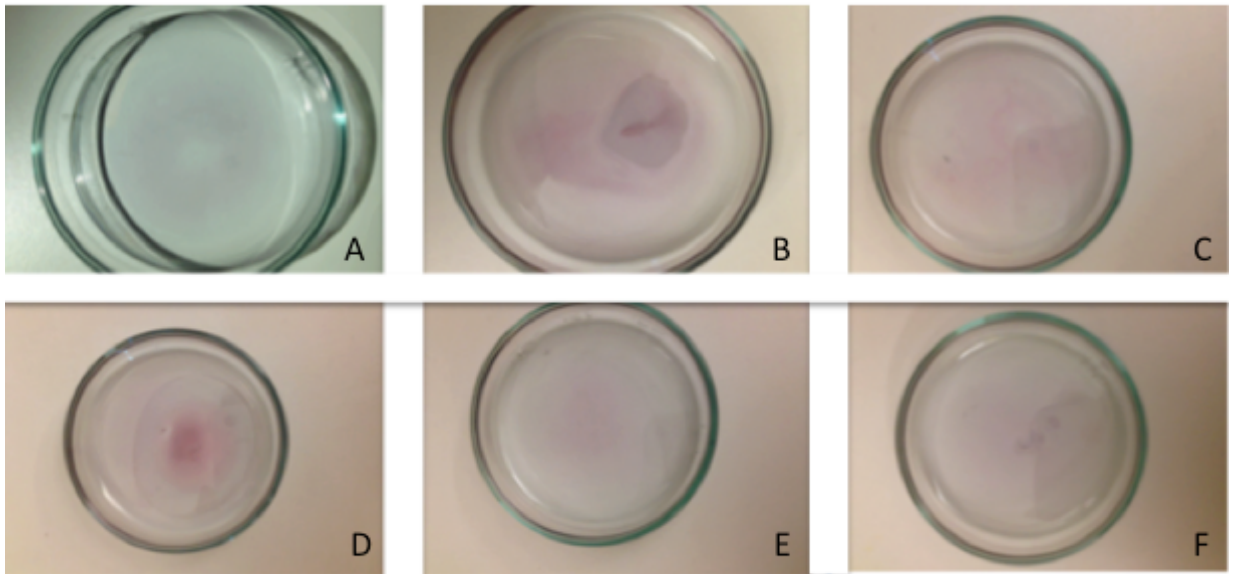


Figure 13. The top row from left to right: BSA in H<sub>2</sub>O (A), BSA in PBS (B) and BSA in TRIS (C). The lower row from left to right: Ig G in H<sub>2</sub>O (D), Ig G in PBS (E) and Ig G in TRIS (F). All the samples were deposited during 1 hour containing 100  $\mu$ l liquid.

Here the film of dispersed gold nanoparticle-protein complexes were visible in all six samples. The highest concentration, the sample that showed the most prominent red color, can be seen in BSA in PBS and TRIS. Both of these samples were subjected to spectroscopic evaluation and the result from this is shown in Figure 14. An absorbance peak around 520 nm indicated that there were gold nanoparticles present in the solutions. In the spectroscopic measurements BSA in TRIS gave the highest output but because of evaporation some of the film in the BSA in PBS samples was not dissolved in the solution that was tested. Therefore BSA in PBS was chosen to be used for efficiency experiments in the Aeroid.

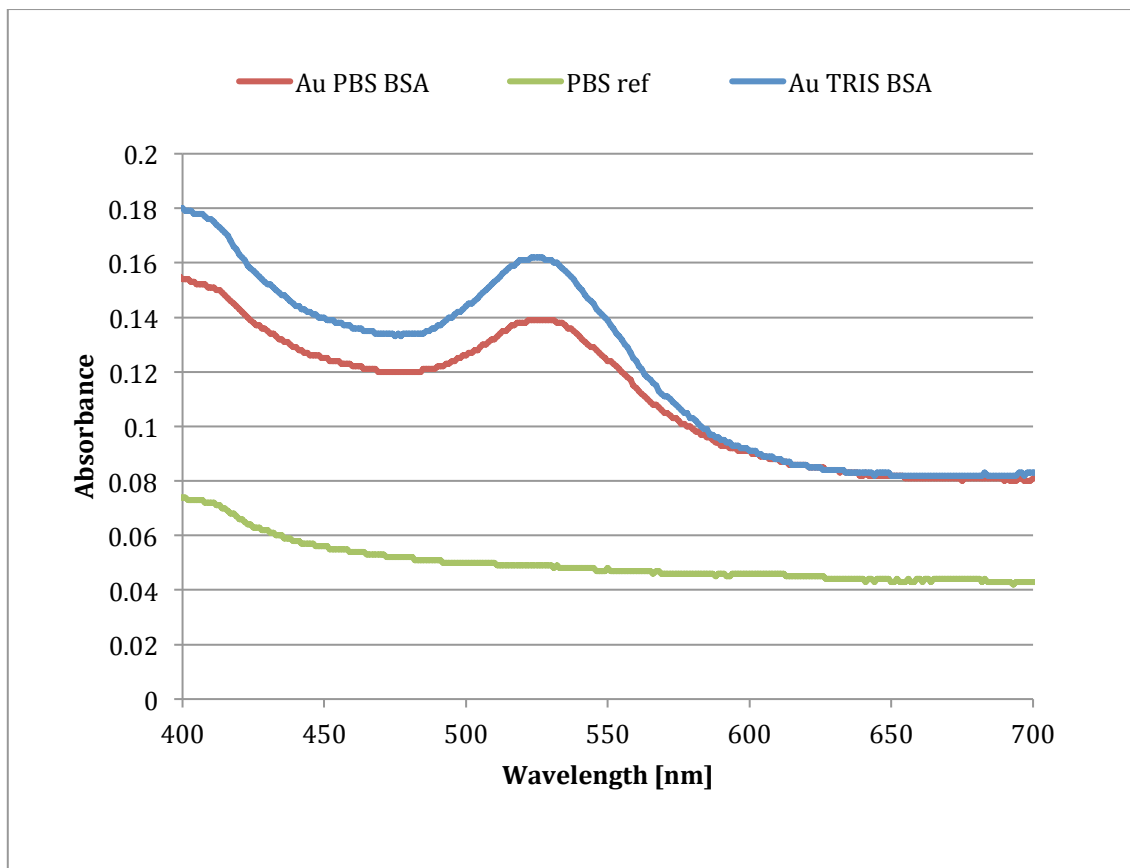


Figure 14 A view of the absorbance peak in a spectroscopy analysis of BSA in PBS, BSA in TRIS and a reference sample with just PBS. Both peaks have a maximum at 520 nm indicating that there is dispersed goldnanoparticles in both samples. A higher peak would suggest a higher concentration of those particles.

### 3.3 Deposition Efficiency Experiment

In the efficiency experiments goldnanoparticles produced by a spark generator where charged by a bipolar charger and deposited in the Aeroid when the the high-voltage was on, this was measured by a SMPS system. To be able to calculate the losses measurements were also done when the the high-voltage unit was off. In Figure 15 the two curves show the size distribution of the aerosol when penetrating the Aeroid when the Aeroid deposition voltages is off and when it is on at 3.5 kV. The difference between the distributions represents what have been deposited inside the Aeroid. Half of the deposited particles will, as mentioned before, have the same charge as the electrode beneath the liquid. Therefore only half of the total amount of charged particles can be deposited in the protein solution due to electrostatic forces.



## Development of wet electrostatic precipitator for generation of nanoparticle-protein solution

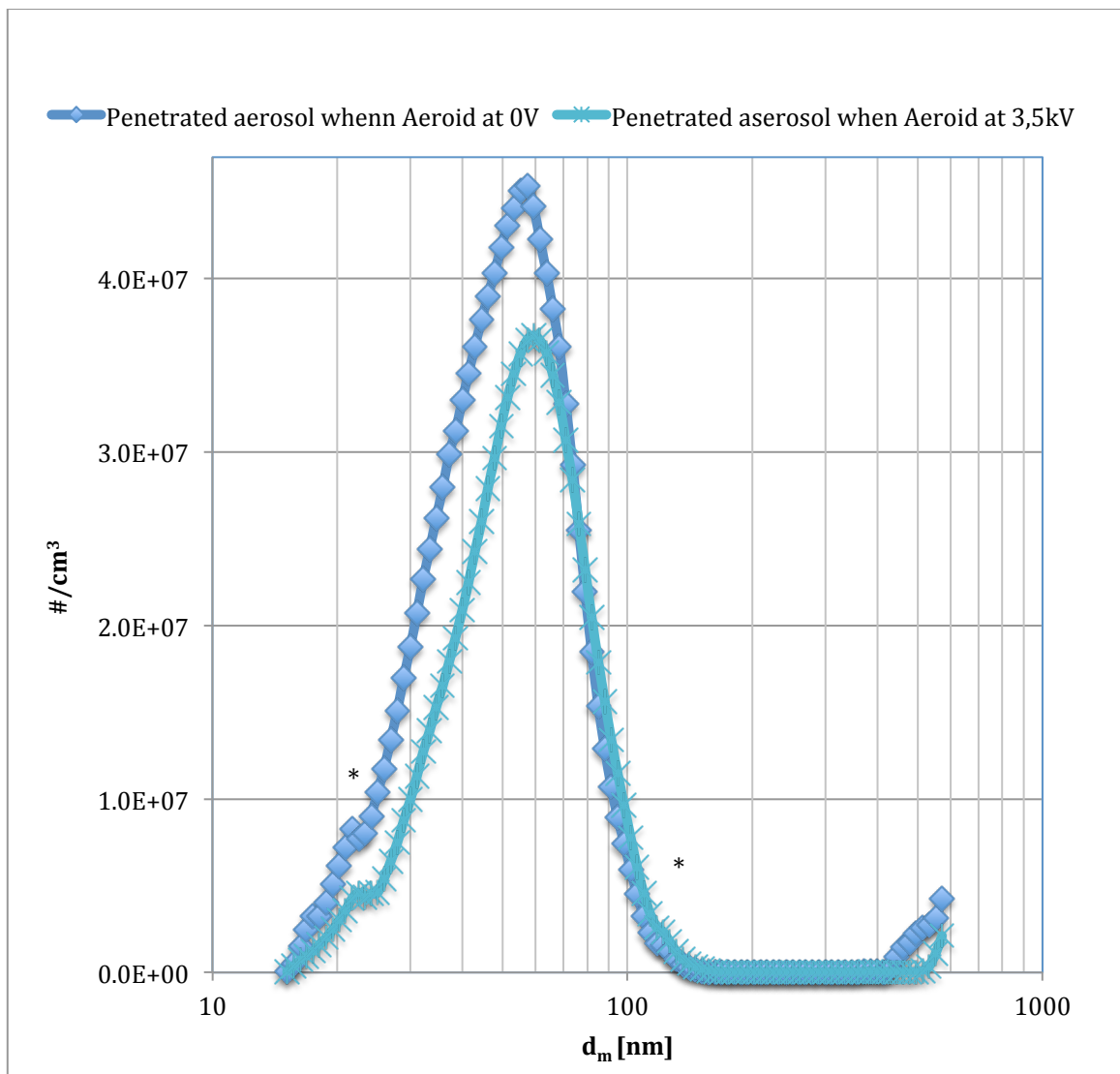


Figure 15 Size distribution of the aerosol penetrate the Aeroid when the high voltage are on at 3,5 kV and of at 0 V measured with a SMPS system. The two stars (\*) mark out where the CPC changes measurement method. The particles that are ionized by a bipolar charger deposit in the Aeroid either on the top electrode connected to the lid or on the surface of the protein solution.

In Figure 15 there are two visible bumps occurring in both curves at 20 nm and at 120 nm, these are marked out with a star (\*) in the Figure 15. These bumps do not belong to the aerosol properties but indicates the shifting of the measurement method for the CPC.

Figure 16 displays the deposited fraction of particles with diameter from 16 to 100 nm. This have been calculated using Eq. 15 in each particle diameter interval. The deposition is at most 30 % around 17 nm and falls steady down to zero at 76%. Also here the bump from the change of measurement method in the CPC can be seen. Particles with a diameter above 76 nm do not seem to deposit. And a negative deposition can be seen at >76 nm this could be because of the fact that the particle concentration goes down at higher diameters and therefore small changes to the system to give false readings.

## Development of wet electrostatic precipitator for generation of nanoparticle-protein solution

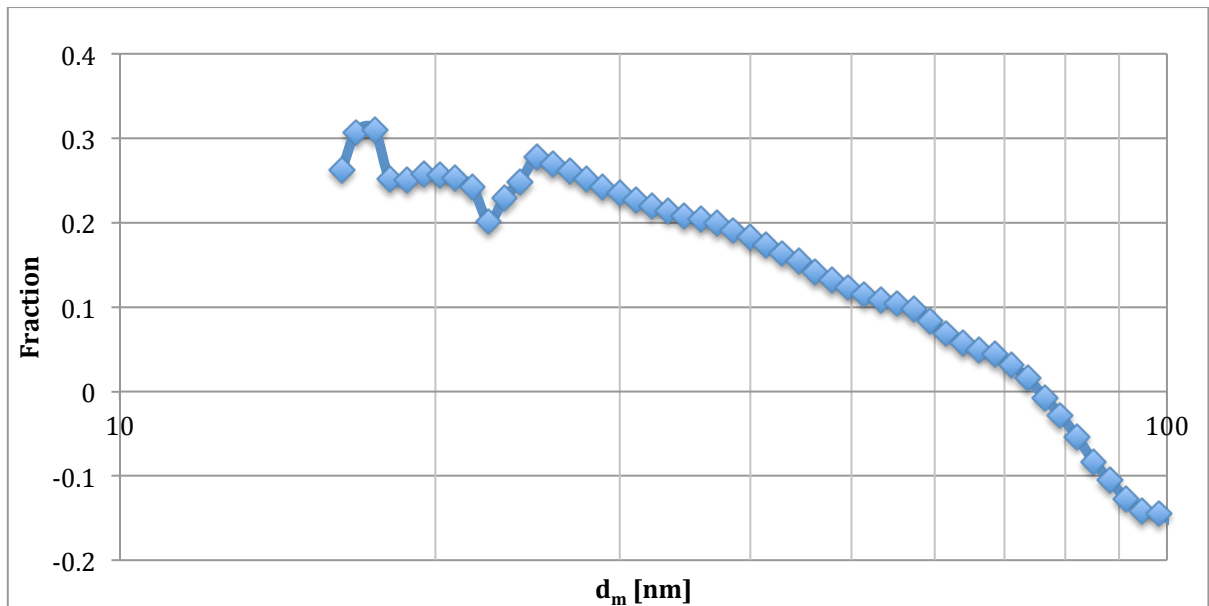


Figure 16 Fraction deposited particles that have been deposited in the solution in the Aeroid between 16 and 76 nm measured with a SMPS system when the high-voltage unit are on at 3,5 kV for three hours.

To be able to calculate the mass concentration in the protein solution, number of particles and total volume were calculated. This was multiplied with the density at  $19.30 \text{ g/cm}^3$  and divided with the volume protein solution, 65 ml, and gave a result of  $11 \text{ }\mu\text{g/ml}$ . The particle concentration were calculated to  $63.4 \cdot 10^7 \text{ \#/ml}$ .

In addition to measurements with SMPS, the protein solutions absorbance was tested in the spectrometer. The results can be seen in Figure 18. Also here we have a peak around 520 nm, indicating dispersed goldnanoparticles but the peak is less pronounced than those seen in Figure 14. This could be because of the lower concentration, but could also mean that the particles are not spherical or have a polydispersed distribution. [30]

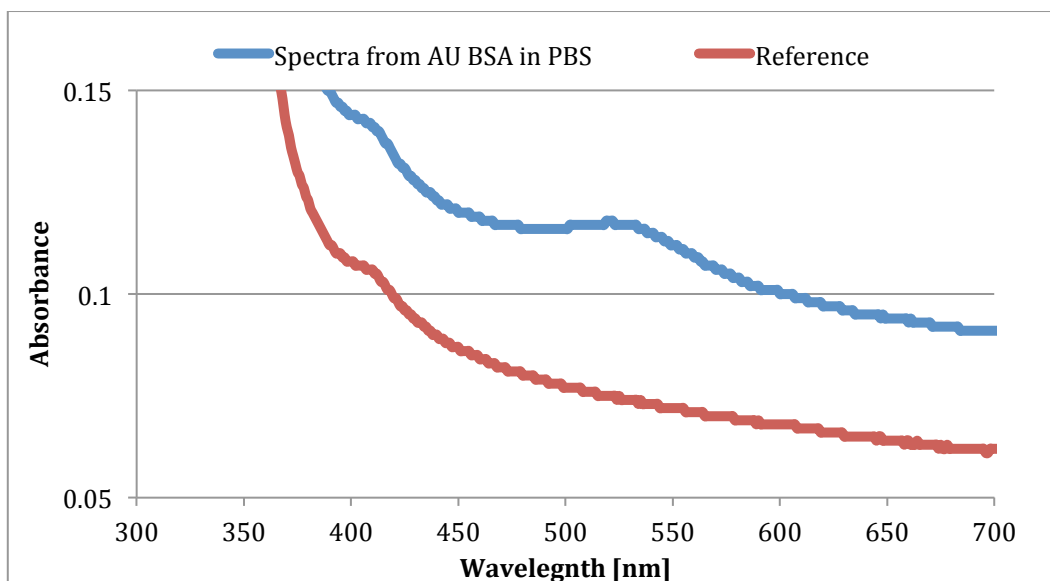


Figure 17 A view of the absorbance peak in a spectroscopy analysis of BSA in PBS and a reference sample with just PBS. The at 520 nm indicating that there is dispersed goldnanoparticles in the samples.

### 3.3.1 Proton Induced X-ray Emission (PIXE)

Filters with dried samples of the goldnanoparticle-protein solution were analysed by PIXE. PIXE is a tool where a beam of protons creates excitations of electrons. When these are falling back into the normal energy level they release an x-ray characteristic of the compound. The intensity of x-rays makes it possible to determine the amount of a compound that is hit by the beam [32].

Three filters with dried samples of 20, 40 and 60  $\mu\text{l}$  solution were sent to be analysed. These came back with 42, 46 and 86 ng respectively. This gave an average concentration of 1.27  $\mu\text{g}/\text{ml}$  with the lowest concentration of 0.91  $\mu\text{g}/\text{ml}$  and the highest at 1.65  $\mu\text{g}/\text{ml}$ . This was approximately a factor 10 below the results calculated from the SMPS data, which could be due to too thick filters.

## 4 Discussion and Conclusions

The overall aim was to create >50 ml colloid suspension of dispersed goldnanoparticles in a protein solution by use of the method developed around a wet electrostatic precipitator. The result showed that this was possible but that the output was low due to losses by diffusion, low charging rate and the use of a bipolar charger.

### 4.1 Discussion

To further develop this method, the problem with losses must be addressed. In average around 30 % of the incoming aerosol is lost due to diffusion in the Aeroid. But the most restricting factor lies in the limits of the bipolar charger where only half of the charged particles will deposit and where a maximum half of the particles will be charged depending on the aerosol characteristics. A unipolar charger would have a much higher throughput of charged particles, and potentially all the charged particles could be deposited on the surface of the liquid in the Aeroid. This would also confine the losses due to diffusion since more particles would be susceptible of the electrical field.

It should be noted that even though a unipolar charger was not used during the experiments, much of the time and resources has been spent on understanding anomalies of one connected to the set up. At the end the charger could not be used because it stopped working completely. In retrospect more time could be spent on measurements without the unipolar charger leaving more reliable data analyses and perhaps a better perspective of the results. Even though the unipolar charger was not used during the experiments it was still connected into the set up and cause losses due to diffusion.

Using a unipolar charger the concentration of charged particles would go up. Adding risk of losses due to that highly charged particles could be more affected by static electricity in the charger and tubes. Another risk of higher particle penetration is the higher risk of aggregation when particles are deposited in the surface of the liquid at the same time. This might be helped by a higher velocity of the recycling liquid.

To improve the exciting system a DMA connected before the Aeroid would single out particles of the desired size interval preventing smaller and larger particles from causing unnecessary diffusion and build up in tubes and charger. This would also allow fine tuning of the strength of the electrical field, in turn leading to less energy consumption, and creating a more uniform colloidal suspension.

Although BSA was the most promising to deliver a solution with a high concentration of dispersed goldnanoparticles, a film was formed on all six samples indicating that it would be possible to use also those in the Aeroid since the method for deposition is the same. Experiments with an ESP have shown to give a good estimation whether the solution would work in the Aeroid and should be used complementary to the Aeroid in a cost effective way for determining if particles or/and biological fluid can provide the desired results.

Spectroscopy of the colloidal goldnanoparticles in protein solution in Figure 18 showed a broad less pronounced peak around 520 nm compared to the peaks in Figure 14. This could

be an effect of the inconsistencies seen in the spark generator creating a broader span of particles. Further investigation for this matter is needed.

### 4.2 Conclusions

The goal to produce a 50 > ml protein solution with dispersed goldnanoparticlecomplexes was achieved. Concentration of the solution probably lies between a factor 10 to a factor 100 less compared to a commercial product without surfactants in PBS [33]. However there is good potential to increase the concentration of particles by a number of methods. But the real strength in the Aeroid lies not in the concentration of particles but in the ability to deposit particles directly into a biological system. In this project bovine serum albumin (BSA) in phosphate buffered saline (PBS) was used but perhaps in the future it will be possible to deposit particles in a solution of blood plasma in the Aeroid. This would have the advantages of immediately giving the particles a biological identity.

Spectroscopy shows a clear indication that there are unaggregated gold particles BSA in PBS. It seems also possible to verify by use of an ESP whether or not a protein solution can work in the Aeroid.

Even though some design parameters ought to be altered, the principal of the overflowing water and the pump system have prevented the formation of a film of stagnated goldnanoparticle-protein complexes. It should also be noted that the color of the end product was even and that no accumulations of complexes were seen in the Aeroid while producing the solution.

Particle measurements show that the deposition efficiency of goldnanoparticles into the liquid is most limited by the amount of ionized particles. This indicates that a higher output of charged particles would increase the efficiency of the Aeroid.

#### 4.2.1 Outlook

This project was an experimental project to test if the idea behind the Aeroid worked. As it did the next step would be to answer the question "Who is going to use the Aeroid?". Depending on the target group changes satisfying the need for that purpose should be made. Further work could include testing different types of particles and solutions.

In all cases a unipolar charger would be the best alternative. But another solution to minimize losses would be to have two basins where one is over the positive electrode and one over the negative electrode. The aerosol would then be led in the middle of the two basins and charged particles would deposit on the basins. To prevent losses a recycling of the uncharged particles would be needed. This would mean more losses due to diffusion than if a unipolar charger was used but increase the efficiency.

## Development of wet electrostatic precipitator for generation of nanoparticle-protein solution

---

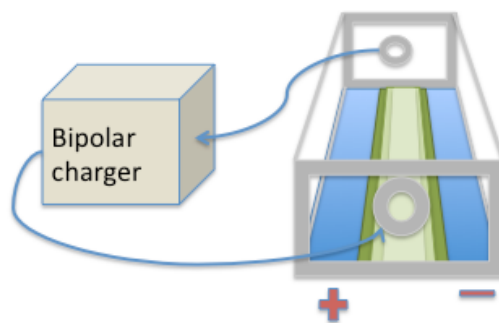


*Figure 18 To be able to increase the efficiency in the Aeroid when using a bipolar charger, a recycling aerosol needs to be used. The arrows represent aerosol going in and out into the Aeroid. The blue lines represent the liquid, below the liquid lies an electrode represented by a + or -.*

## 5 References

1. Salata OV. (2004). Applications of nanoparticles in biology and medicine. *Journal of Nanobiotechnology* 2(3)
2. Geriano L, Heuberger M, Nowack B. (2009). The behavior of silver nanotextiles during washing. *Environmental Science and Technology* 43:8113-8118
3. Nowack B., Bucheli T.D. (2007). Occurrence, behavior and effects of nanoparticles in the environment, *Environmental Pollution*, 150(1): 5–2
4. Hinds (1999) *Aerosol Technology*, Second Edition, John Wiley & Sons, Chapter 11, Chapter 15-31 and Chapter 7
5. Lynch, I., Salvati, A., & Dawson, K. A. (2009). Protein-nanoparticle interactions: what does the cell see?. *Nature nanotechnology*, 4(9): 546-547
6. Miyabara Y, Yanagisawa R, Shimojo N, Takano H, Lim HB, et al (1998) Murine strain difference in airway inflammation caused by diesel exhaust particles. *Europe Respiratory Journal* 11: 291-298
7. Tippe A., Heinzmann U., Roth C. (2002) Deposition of fine and ultrafine aerosol particles during exposure at the air/cell interface. *Journal of Aerosol Science* 33(2):207-218. Doi: 10.1016/S0021-8502(01)00158-6
8. Svensson CR, Messing ME, Lundqvist M, Schollin A, Deppert K, et al (2013) Direct Deposition of Gas Phase Generated Aerosol Gold Nanoparticles into Biological Fluids – Corona Formation and Particle Size Shifts. *PLOS ONE* 8(9): e74702. doi:10.1371/journal.pone.0074702
9. Lagzi, Mészáros, Gelybó, Leelőssy *Atmospheric Chemistry* (2013) <<http://elte.prompt.hu/sites/default/files/tananyagok/AtmosphericChemistry/ch09s02.html>> (2015-06-11)
10. C. Isaxson, *Introduction to Aerosols* (2014) <<http://luvit.ced.lu.se/LuvitPortal/education/main.aspx?courseid=5816>> (2015-06-15)
11. Raaschou-Nielsen O., Andersen, Z.J., Beelen R., Samoli, E., Stafoggia M., Weinmayr G., Hoffmann B., Fischer P., Nieuwenhuijsen M.J., Brunekreef B., Xun, W.W., Katsouyanni K., Dimakopoulou K., Sommar J., Forsberg B., Modig L., Oudin A., Oftedal B., Schwarze P.E., Nafstad P., De Faire U., Pedersen N.L., Östenson C.G., Fratiglioni L., Penell J., Korek M., Pershagen G., Eriksen K.T., Sørensen M., Tjønneland A., Ellermann T., Eeftens M., Peeters P.H., Meliefste K., Wang M., Bueno-de-Mesquita B., Key T.J., de Hoogh K., Concin H., Nagel G., Vilier A., Gironi S., Krogh V., Tsai M.Y., Ricceri F., Sacerdote C., Galassi C., Migliore E., Ranzi A., Cesaroni G., Badaloni C., Forastiere F., Tamayo I., Amiano P., Dorronsoro M., Trichopoulou A., Bamia C., Vineis P., Hoek Gerard. (2013) Air pollution and lung cancer incidence in 17 European cohorts: prospective analyses from the European Study of Cohorts for Air Pollution Effects (ESCAPE) *In Lancet Oncology* 14(9):813-822. DOI: 10.1016/S1470-2045 (13)70279-1,
12. Dockery D.W. (2009). Health Effects of Particulate Air Pollution, *Annals of Epidemiology* 19(4): 257-263.
13. Hagerman I., Isaxson C., Gudmundsson A., Wierzbicka A., Dierschke K., Berglund M., Pagels J., Nielsin J., Assarson E., Andersson U. B.K, XU Y., Jönsson B. A.G., M. Boghard (2013), Effects on Heart Rate Variability by Artificially Generated Indoor Nano-sized Particles in a Chamber Study, *Atmospheric Environment* 88: 165-171
14. Seiffert J, Hussain F, Wiegman C, Li F, Bey L, Baker W, et al. (2015) Pulmonary Toxicity of Instilled Silver Nanoparticles: Influence of Size, Coating and Rat Strain. *PLoS*

ONE 10(3): e0119726. Doi: 10.1371/journal.pone.0119726

15. Salvati A., Pitek A.S., Monopoli M.P., Prapainop K., Bombelli F.B., Hristov D.R., Kelly P.M., Åberg C., Mahon E., Dawson K.A. (2013) Transferrin-functionalized nanoparticles lose their targeting capabilities when a biomolecule corona adsorbs on the surface. *Nature Nanotechnology* 8 (2), 137-143. DOI: 10.1038/nnano.2012.237
16. Altman R., Offen G., Buckley W., and Ray I. (2001a) Wet Electrostatic Precipitation: Demonstrating Promise For Fine Particulate Control – Part I Power Engine 105:37-39 and Part II Power Engine 105:42-44
17. Dey L. and Venkataraman C. (2012) A Wet Electrostatic precipitator (WESP) for Soft Nanoparticle Collection, *Aerosol Science and Technology*, 46(7): 750-759, DOI: 10.1080/02786826.2012664295
18. Lin G.Y., Tsai C.J., Chen S.C., Chen T.M. and Li S.N. (2010) An Efficient Single-Stage Wet Electrostatic Precipitator for Fine and Nanosized Particles Control, *Aerosol Science and Technology*, 44(1): 38-45, DOI: 10.1080/02786820903338298
19. Baron P.A., Kulkarni P., Willeke K. (2011) *Aerosol Measurement; Principles, Techniques, and Applications*, Second Edition, John Wiley & Sons, Inc
20. Allen M., and Raabe O. (1985). Slip correction measurements of spherical solid aerosol particles in an improved Millikan apparatus. *Aerosol Science and Technology*. 4(3): 269–286
21. Baron P.A., P. Kulkarni and K. Willeke (2011) *Aerosol Measurement: Principles, Techniques, and Applications*, Third Edition, John Wiley & Sons, Inc.
22. Gunn R.(1956) Measurements Related to the Fundamental Processes of Aerosol Electrification. *Journal of Colloid Science*. 11, 661.
23. Fuchs N.A. (1963) On the stationary charge distribution on aerosol particles in a bipolar ionic atmosphere. *Geofisica Pura e Applicata* 56(1): 185-193.
24. Wiedensohler A. (1988) An approximation of the bipolar charge distribution for particles in the submicron size range. *Journal of Aerosol Science*. 19:3, 387-389
25. Tommy Cedervall , Iseult Lynch , Stina Lindman, Tord Berggård, Eva Thulin, Hanna Nilsson, Kenneth A. Dawson and Sara Linse (2006) Understanding the nanoparticle–protein corona using methods to quantify exchange rates and affinities of proteins for nanoparticles, *PNAS* 104(7);, 2050-2055.
26. Product information Sigma-Aldrich (2000)  
<[http://www.sigmaaldrich.com/content/dam/sigmaaldrich/docs/Sigma/Product\\_Information\\_Sheet/b4287pis.pdf](http://www.sigmaaldrich.com/content/dam/sigmaaldrich/docs/Sigma/Product_Information_Sheet/b4287pis.pdf)> (2015-06-18)
27. Junqueira L.C., Jose Carneiro (2003). *Basic Histology*. McGraw-Hill. ISBN 0-8385-0590-2
28. Product information Thermo Scientific  
<<http://www.thermoscientific.com/content/dam/tfs/LPG/LCD/LCD%20Documents/Catalogs%20&%20Brochures/Microplate%20Instrumentation/Microplate%20Readers/D01621~.pdf>> (2015-06-10)
29. Hollas M.J (2004) *Modern Spectroscopy* Fourth Ed. John Wiley and Sons Ltd  
<[http://optdesign.narod.ru/book/Hollas\\_Modern\\_spectroscopy.pdf](http://optdesign.narod.ru/book/Hollas_Modern_spectroscopy.pdf)> (2015-06-18)
30. Turkevich J., Garton G., Stevenson P.C. (2004) The color of colloidal gold, *Journal of Colloid Science* 9:1, 26-35
31. ESP Design Parameters and Their Effects on Collection Efficiency, chapter 3 (2015)  
<[https://www.neundorfer.com/FileUploads/CMSFiles/ESP%20Design%20Parameters\[0\].pdf](https://www.neundorfer.com/FileUploads/CMSFiles/ESP%20Design%20Parameters[0].pdf)> (2015-06-15)
32. Johansson and John L. Campbell and Klase G Malmöqvist (1997). Particle-induced



## Development of wet electrostatic precipitator for generation of nanoparticle-protein solution

---

X-ray emission Spectrometry 26(1): 49-50 (PIXE), ISBN 0-471-58944-6

33. Gold Nanoparticles: Properties and Applications (2015)

<<http://www.sigmaaldrich.com/materials-science/nanomaterials/gold-nanoparticles.html>>

(2015-06-18)